

An optical Bragg scattering readout for simultaneous detection of all low-order mechanical modes of gallium nitride nanowires in nanowire arrays¹

*John P. Houlton^{*1}, Matt D. Brubaker², Kris A. Bertness², and Charles T. Rogers¹*

¹Department of Physics, University of Colorado, Boulder, Colorado 80309, USA

²National Institute of Standards and Technology, Boulder, Colorado 80305, USA

We report the use of optical Bragg scattering and homodyne interferometry to simultaneously measure all the first order cantilever-mode mechanical resonance frequencies and quality factors (Q) of gallium nitride nanowires (GaN NWs) in 100 NW periodic selected-area growth arrays. Hexagonal 2D arrays of 100 GaN NWs with pitch spacings of 350-1100 nm were designed and prepared to allow optical Bragg scattering. The NWs studied have diameters ranging from 100-300 nm, lengths from 3-10 μm , resonance frequencies between 1-10 MHz, and Q-values near 10,000 at 300 K. The system can passively detect the thermally induced Brownian mechanical motion of the NWs and can study driven NW motion, enabling the simultaneous monitoring of hundreds of mechanical resonators in a 10-100 μm^2 area with a single optical beam. The read-out system allows large arrays of NWs to be characterized and applied as e.g. spatially resolved temperature and mass sensors.

Keywords: nanowires, nano-mechanical systems, complex nanostructures, III-V semiconductors.

Nano-mechanical resonators are interesting and potentially useful as extremely small and sensitive detectors of mass, force, temperature, and pressure and as clocks and possible components of quantum information systems.¹⁻⁵ *c*-axis oriented gallium nitride nanowires (GaN NWs) are particularly interesting due to their unusually low mechanical dissipation and associated high quality factors, Q (defined as the ratio of the resonator's center frequency and lineshape full-width at half-maximum power), and have been shown to be useful for a host of

¹ Contribution of an agency of the U.S. government; not subject to copyright.

high-resolution sensing applications.⁵⁻⁹ Recent progress¹⁰ on selected-area growth of GaN NWs allows accurate lithographic positioning of NWs and lithographic control of NW diameters. In this letter, we report the fabrication and performance of periodic GaN NW arrays that are designed to produce coherent optical scattering (Bragg scattering) in selected directions. Since the optical scattering from all the NWs in the array is of the same phase in these special directions, collection of the light and optical homodyne interferometry then allows the simultaneous detection of mechanical motion of hundreds of NW vibrational modes.

The GaN NWs studied in this work were grown on Si (111) wafers using catalyst-free, plasma-assisted molecular beam epitaxy (MBE).¹¹ Layers of $[000\bar{1}]$ oriented AlN and GaN are grown on top of a Si substrate. A silicon nitride (SiN_x) mask layer is deposited and patterned with periodic arrays of holes, allowing for the control of NW diameter and spacing. Selective-area growth of GaN NWs occurs in a subsequent growth step.^{10,11} The resulting NWs are long columnar single-crystals, hexagonal in cross-section and are epitaxially anchored to the substrate with their c -axis oriented along the long axis of the NW and perpendicular to the growth substrate. An example of one of these NW arrays is shown in tilted and plan views in Figures 1a and 1b respectively.

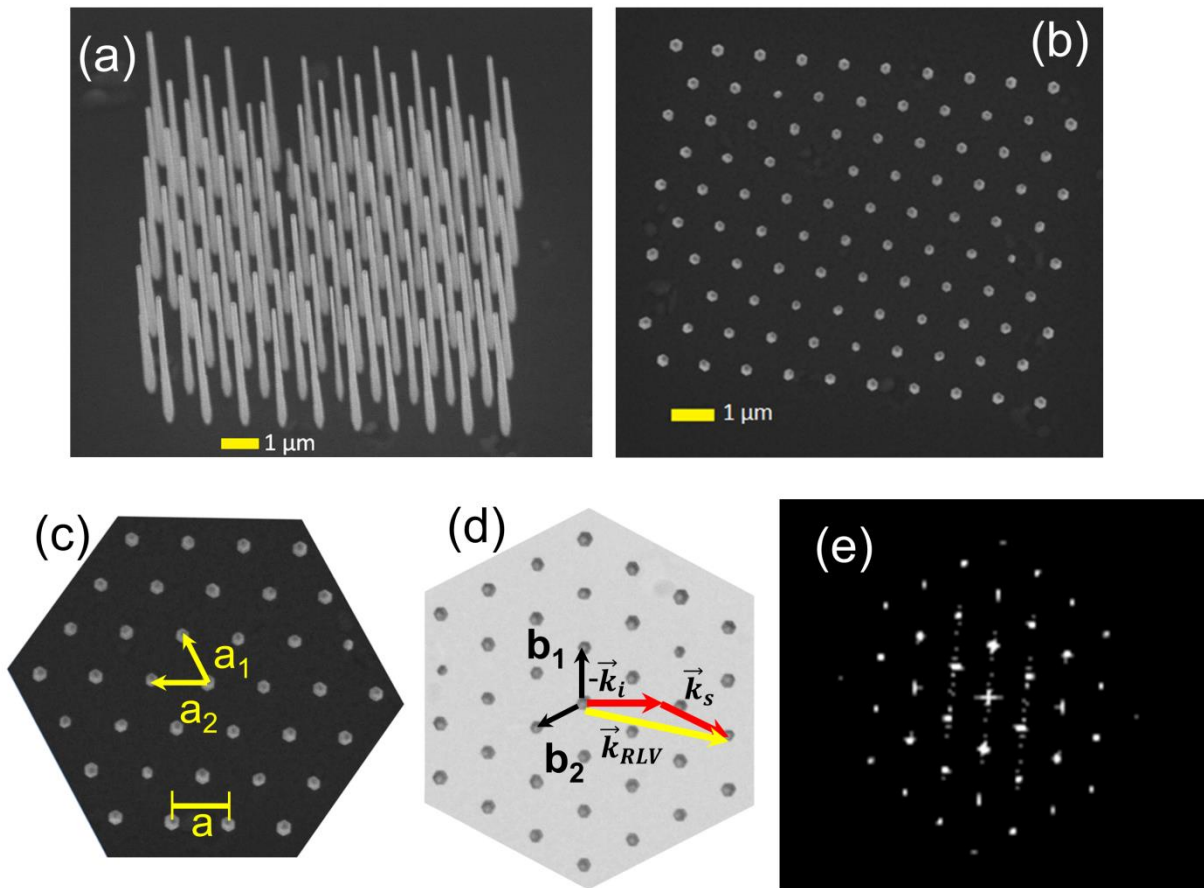


Figure 1. (a) (b) SEM images of a representative array of GaN NWs selectively grown in a hexagonal lattice pattern shown with 25 degree tilt and plan view respectively. The scale bars are each 1 μm . The NWs in this array have typical lengths of 8 μm and tip diameters of 120 nm. Additionally, the NWs in this array exhibit non-uniform diameters along their lengths. (c) Segment of the SEM image from (b) highlighting the NW array's appearance as a 2D hexagonal lattice. The nearest neighbor spacing, a , is designed to be 1012 nm. Primitive vectors, a_1 and a_2 , for the 2D lattice are shown. (d) Diagram showing a portion of the reciprocal space corresponding to an infinite 2D hexagonal real space lattice. Primitive reciprocal vectors, b_1 and b_2 , are shown. An example of coherent, elastic optical scattering into diffraction order (-2, -3) is shown schematically. The difference between the incident and scattered light k vectors is equal to a reciprocal lattice vector. (e) 2D FFT computed from the SEM image in (b), showing good agreement with the simple infinite 2D lattice model. The fine structure around the lattice points in (e) are due to finite size effects and defects within the NW array.

The as-grown NWs in the studied arrays have typical lengths of roughly 10 μm and diameters of order 100 nm and have Young's modulus of about 300 GPa.¹² The NWs function as singly-clamped cantilever mechanical resonators with typical lowest-order mechanical frequencies in the 1-10 MHz range and Qs on the order of 10,000 at 300 K. For NWs with perfect hexagonal cross-sections, the two lowest-order normal modes are degenerate in frequency. However, due to small asymmetries in NW structure, this degeneracy is lifted, and two distinct lowest-order flexural modes are expected.^{6,7} An array containing 100 NWs is expected to contain an ensemble of 200 lowest-order resonances, and a large number of pairs of higher-order vibrational modes.

We use optical interferometry to read out the mechanical motion of NWs. Optical interferometry has been previously used in the study of nano-mechanical systems and NWs in particular.¹³⁻¹⁵ It is an appealing technique as it provides a non-contact, *in-situ* measurement without the need for added sample fabrication steps and has a very low risk of damaging the NWs or modifying their mechanical properties.

We use a helium neon (HeNe) laser operating at 632.8 nm and 5 mW of optical power as the primary light source in our optical detection system. The approximately TEM_{00} output of the laser is expanded to a 1 cm diameter collimated beam and then focused to a measured beam waist radius, $w_0 = 3 \mu\text{m}$. Arrays of GaN NWs are then placed in the beam waist such that the long axis of the NWs is perpendicular to the optical propagation direction, \vec{k}_i in Figure 1d, of the incident laser light (grazing optical incidence to the substrate). The linear polarization of the laser light is parallel to the long axis of the NWs to maximize their scattering efficiency. Light scattered from the NWs is collected and interfered with a reference wave taken from the same laser source. We have used a variety of experimental geometries to achieve this optical

interference. These include using a Mach-Zehnder interferometer with the NW array in the sample arm, using interference between the incident Gaussian beam and forward scattered light from NWs,¹⁶ and using interference between NWs' stationary bases and moving ends by a slight tilt of the incident light's phase front relative to the NWs' long axis. With the proper 90 degree phase relationship between the chosen reference wave and the scattered wave from a moving NW, motion of sections of the NW along the direction of the scattered light, \vec{k}_s in Figure 1d, results in a linear response modulation of the intensity of the combined light field. This light intensity is monitored by a low-noise photodetector system with a 10 MHz electronic bandwidth. The photodetector signal is then studied as desired e.g. by time record or Fourier analysis to detect the motion of the NW mechanical resonators.

To simultaneously detect the motion of multiple NWs in a single interferometric measurement, as would be favorable for sensing applications, it is necessary that the scattered light from each NW have the same phase difference relative to the reference wave. That is, one would desire phase coherent scattering from an ensemble of NWs. We achieve this coherent optical scattering from a periodic array of ~100 NWs by designing the spacing between NWs in the array, to produce a 2D photonic crystal that Bragg scatters 632.8 nm light in a selected direction. Optical Bragg scattering from arrays of Si NWs for color generation and refractometric sensing has been previously demonstrated.^{17,18}

The design of our Bragg scattering GaN NW arrays is guided by simple crystal lattice scattering theory.¹⁹ Figure 1b shows a top-down view of a 1012 nm pitch NW array which appears as portion of a 2D hexagonal real-space crystal lattice. All possible linear combinations of the primitive vectors, \mathbf{a}_1 and \mathbf{a}_2 (see Figure 1c), would be used to generate an ideal infinite lattice. The reciprocal, or k-space, lattice is determined by taking the 2D spatial Fourier transform of this real-space lattice. Figure 1d shows a portion of the reciprocal space corresponding to the ideal real space lattice. This reciprocal space lattice shares the same 6-fold rotational symmetry as the real space lattice and is rotated 60 degrees relative to it. The lengths of the primitive reciprocal vectors, \mathbf{b}_1 and \mathbf{b}_2 , are inversely related to \mathbf{a}_1 and \mathbf{a}_2 by:

$$|\mathbf{b}| = \frac{4\pi}{\sqrt{3}|\mathbf{a}|}, \quad (1)$$

and an infinite reciprocal space lattice can be similarly generated from all linear combinations of \mathbf{b}_1 and \mathbf{b}_2 . Each particular linear combination is known as a reciprocal lattice vector, \vec{k}_{RLV} . When light with wavevector, \vec{k}_i , is incident on a crystal lattice it will be coherently scattered into an

outgoing wave with wavevector, \vec{k}_s , only when the difference between the incident and scattered wavevectors is equal to a reciprocal lattice vector of the crystal. That is, the Laue condition,

$$\vec{k}_s - \vec{k}_i = \vec{k}_{RLV}, \quad (2)$$

must be satisfied. Additionally, the GaN NWs scatter light elastically, and so, $|\vec{k}_i| = |\vec{k}_s|$.

An example of coherent scattering is shown schematically in Figure 1d. The 632.8 nm light used in this experiment has $|\vec{k}| = \frac{2\pi}{\lambda} = 9.93 \mu\text{m}^{-1}$. For the example array, $|\mathbf{a}| = 1012 \text{ nm}$, i.e., $|\mathbf{b}| = 7.17 \mu\text{m}^{-1}$, we scatter off the reciprocal lattice point shown in the diagram. For this example, coherent backscattering at about 150 degrees to the incident laser light (or \vec{k}_s is about 30 degrees below $-\vec{k}_i$ in Figure 1d) is achieved at a particular sample orientation. If we were to change the spacing of NWs in the array, the spacing of the reciprocal lattice points would also change, according to Equation 1. To scatter from the same reciprocal lattice point, the orientations of \vec{k}_i and \vec{k}_s must change, leading to a different coherent backscattering angle. We computed the backscattering angle (for particular reciprocal lattice vectors) as a function of array pitch in the case of an infinite 2D lattice for pitches varied around 400 nm (diffraction index (1,0)), 700 nm (diffraction index (2,1)), and 1000 nm (diffraction index (-2,-3)), as shown in Figure 2. GaN NW arrays were then grown with 15 different pitch values, and optical scattering experiments were performed to determine each design's coherent backscattering angle in the plane of the sample substrate. The physical arrays, though finite in size and containing some defects (usually a small number of missing NWs), performed close to the simple theory predictions, as seen in Figure 2.

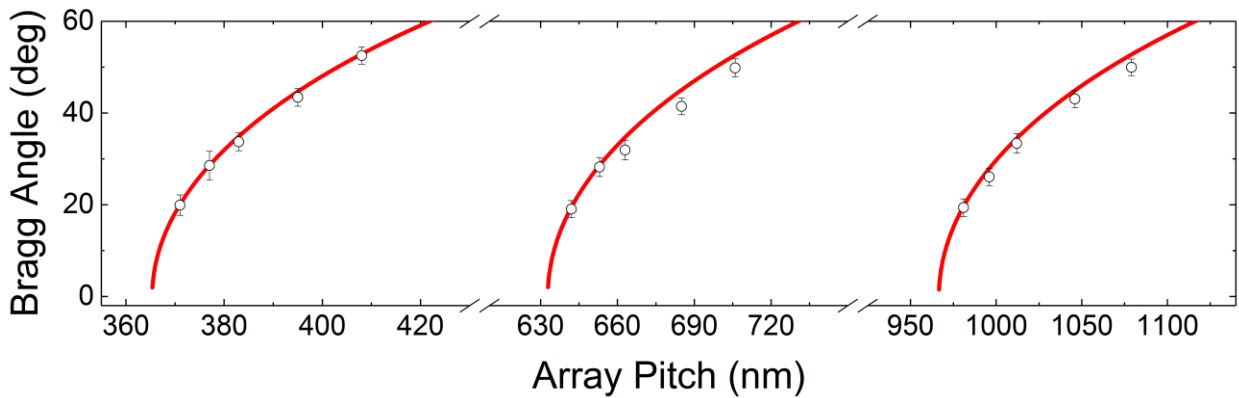


Figure 2. Plots showing the coherent backscattering angle (the angle between \vec{k}_s and $-\vec{k}_i$ in Figure 1d) for 632.8 nm HeNe laser light as a function of the nominal designed nearest neighbor spacing or pitch between NW sites in hexagonal array structures, for pitches varied near 400 nm (diffraction index (1,0)), 700 nm (diffraction index (2,1)), and 1000 nm (diffraction

index (-2, -3)). The solid red curves are theoretical predictions modeling NW arrays as simple infinite 2D lattices of point scatterers. The data points show the measured Bragg angles for 10 x 10 NW arrays prepared with 15 different pitch values.

We studied the coherent backscattered light from NW arrays held in a helium cryostat under a 4×10^{-4} Pa vacuum. Our system is routinely capable of observing all the lowest-order mechanical modes in a given NW array using only the thermally induced Brownian motion of the NWs i.e., without the application of any drive. This passive detection scheme allows us to quickly characterize ensembles of hundreds of low-order mechanical modes. We also regularly observe higher-order bending modes out to the maximum frequency of the photodiode amplifier. Each NW is a harmonic oscillator coupled to a finite temperature bath, and each resonance is therefore expected to have a thermal deflection spectral density given by the Lorentzian lineshape²⁰

$$S_x(\omega) = \left(\frac{4k_B T}{MQ} \right) \frac{\omega_0}{(\omega_0^2 - \omega^2)^2 + \left(\frac{\omega_0^2}{Q} \right)^2}, \quad (3)$$

where k_B is the Boltzmann constant, T is the temperature of the NW, $\omega_0 = 2\pi f_0$ is the NW resonance frequency (in rad/sec), M is the effective mass of the NW, and Q is the quality factor of the resonator lineshape. Integrating Equation 3 over all frequency gives a mean squared resonator deflection, $\langle x^2 \rangle = \frac{k_B T}{M\omega_0^2}$, a statement of the equipartition theorem for a harmonic oscillator. The NWs studied here have nominal rms deflections at 300 K of ~ 0.1 nm.

The transduction of each individual NW's deflection into detectable signal in our system will depend on the details of the NW's optical scattering efficiency and the orientation of the resonance's modal motion relative to the interferometer axis. A distribution of detection efficiencies is therefore expected for the resonances in a given array. Figure 3a shows a typical power spectral density (PSD) measurement of the thermal motion of NWs in an array. This dense set of noise peaks is a fingerprint unique to the specific NW array from which the data was taken. Figure 3b shows a small region of frequency space near 2.59 MHz to more clearly show one of the thermal Lorentzian resonance peaks we observed. Once the NW resonances in an array have been found through thermal motion and catalogued, NWs can be further studied by purposely driving their resonant motion. We drive NW motion by applying rf modulated heat pulses to the sample substrate near NW arrays using a focused 405 nm laser.¹⁴ Figure 3c shows an example of a lock-in measurement performed by sweeping the modulation frequency of the blue laser through the NW resonance near 2.59 MHz. The in-phase and quadrature response of the lock-in are recorded and simultaneously fitted with a two component complex Lorentzian function in order to extract and track NW center frequency and quality factor.^{6,20}

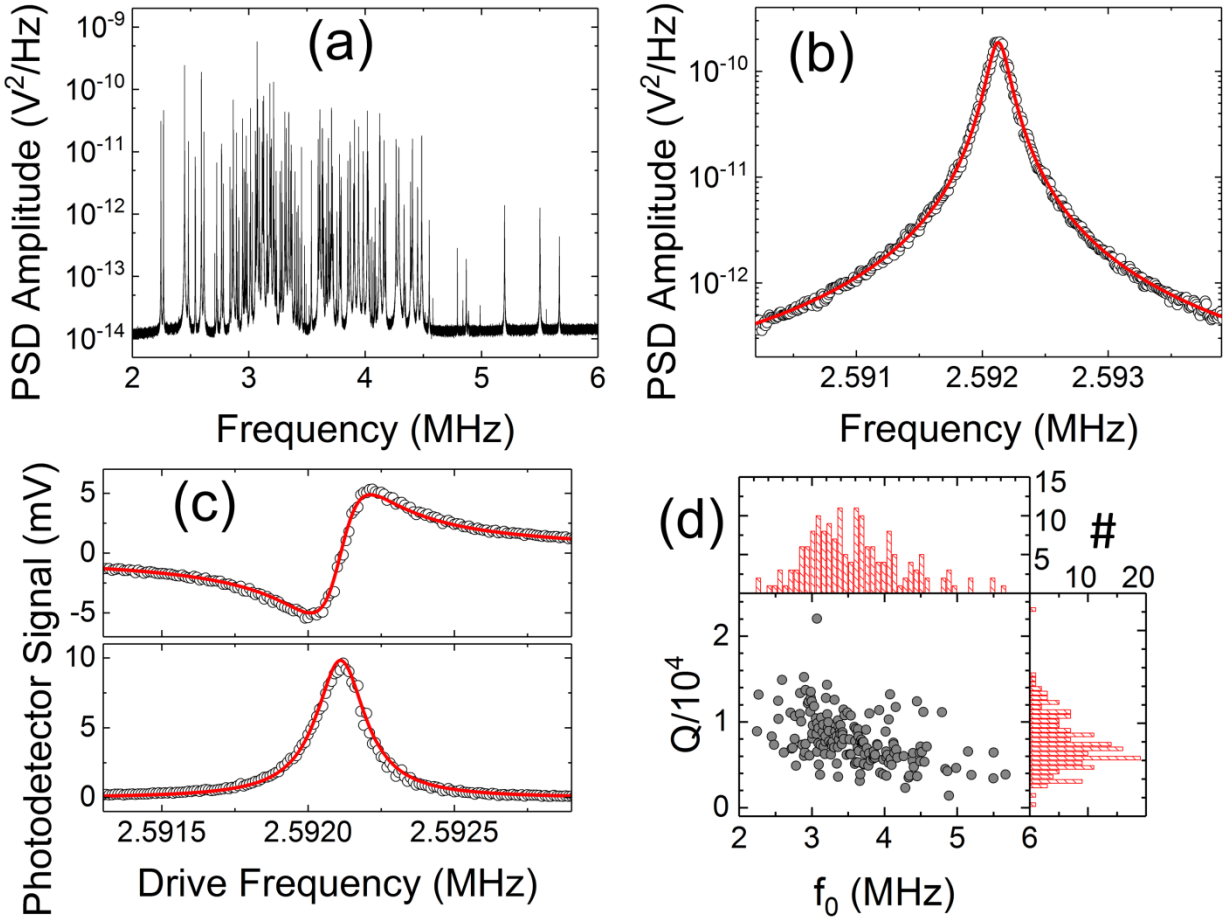


Figure 3. (a) A thermal noise power spectral density (PSD) for an ensemble of resonances from a 653 nm pitch array of NWs at 390 K. This style of measurement allows for the simultaneous detection of all lowest-order mechanical modes in the array (typically 100 – 200 modes). (b) A close look at a frequency region showing a single thermal noise peak of a NW. The solid red curve is a Lorentzian fitting of the data with a resonance frequency, $f_0 = 2,592,127.1 \pm 0.4$ Hz, a width $\Delta f = 173 \pm 1$ Hz, and a mechanical quality factor, $Q = 15,000 \pm 100$. (c) The same NW resonance in driven response as measured by an rf lock-in amplifier. The top plot shows the in-phase response of the oscillator, and the bottom plot shows the quadrature response. The solid red curves are a simultaneous fitting of the data to a two component Lorentzian function. (d) Scatter plot and histograms of all 170 center frequencies and Qs of NW resonance peaks fitted from the PSD measurement in (a).

Figure 3d shows examples of information that can be quickly extracted from a thermal PSD measurement of an array of NWs. The plot shows the fitted center frequencies versus quality factors and accompanying histograms of the thermal resonance peaks in the spectrum shown in Figure 3a. The distribution of center frequencies has a mean value of 3.59 MHz and a standard

deviation of 0.66 MHz. This range of observed peak frequencies is consistent with geometric variations of NWs within the array as measured by SEM imaging and an Euler-Bernoulli beam model for NW resonance frequency.²⁰ The Qs of the resonances observed in this array average around 8,000, with many exceeding 10,000. This measurement was taken at a temperature of 390 K. Upon cooling to below 100 K, resonances typically demonstrate Qs around 30,000. We see a slight downward trend in Q as a function of resonance frequency in the ensemble data, consistent with higher frequency NWs tending to have shorter lengths, L , and/or wider diameters, d , and clamping loss²¹ limited Qs scaling as $(L/d)^3$. These Qs are similar to previously studied GaN NWs grown by random nucleation processes,^{6,8} indicating that the selected-area growth process used here produces NWs of similarly high mechanical quality.

The ability to simultaneously measure resonances from large numbers of nano-resonators opens opportunities for studying the range of variations of resonator properties and for new sensor applications. For example, variable temperature Young's modulus with different NW length and radius gives NWs a temperature coefficient for their resonance frequencies. We have measured $\frac{\partial f_0(T)}{\partial T} / f_0$ for NWs in a 371 nm pitch array in a temperature range of 80-120 K to be linear with temperature with typical values of 23 ppm/K and a spread of values of 9 ppm/K. The NWs in the studied array had nominal diameters of 150 nm and lengths of 9 μm . We find that each NW resonance has a unique and reproducible temperature coefficient. Such arrays can be used as densely packed sets of thermometers for measuring e.g. spatially resolved surface temperature fields.

Also useful for many applications is the operation of NWs as driven oscillators in closed feedback loops. Previous work has shown that individual GaN NWs can be driven into feedback oscillations using SEM based measurements and a shear-mode piezo-actuator drive mechanism.⁶ We regularly use our optical readout signal to drive the heat-pulse-generating laser thus closing a feedback loop to operate NWs as feedback oscillators. Figure 4a shows a thermal PSD from an array of NWs while Figure 4b shows a PSD taken on the same array upon closing this feedback loop. Figure 4c shows a small region of frequency space near 2.59 MHz to more clearly show a NW peak with and without feedback. NW resonance peaks are either enhanced in signal amplitude (with Q sharpened to factors in excess of 10^5) or decreased in amplitude, depending on the overall phase shift they experience in the feedback loop. Figure 4d shows an example time record of the measured optical signal when two resonances are in simultaneous feedback oscillations. A distinct beat note at approximately 200 kHz arises as the feedback oscillations at 2.86 MHz and 3.07 MHz interfere, thus indicating the simultaneous, continuous operation of the two oscillators. The ability to run NW arrays in closed loop oscillation allows for applications such as high signal-to-noise^{2,6,22} and spatially resolved mass sensors.

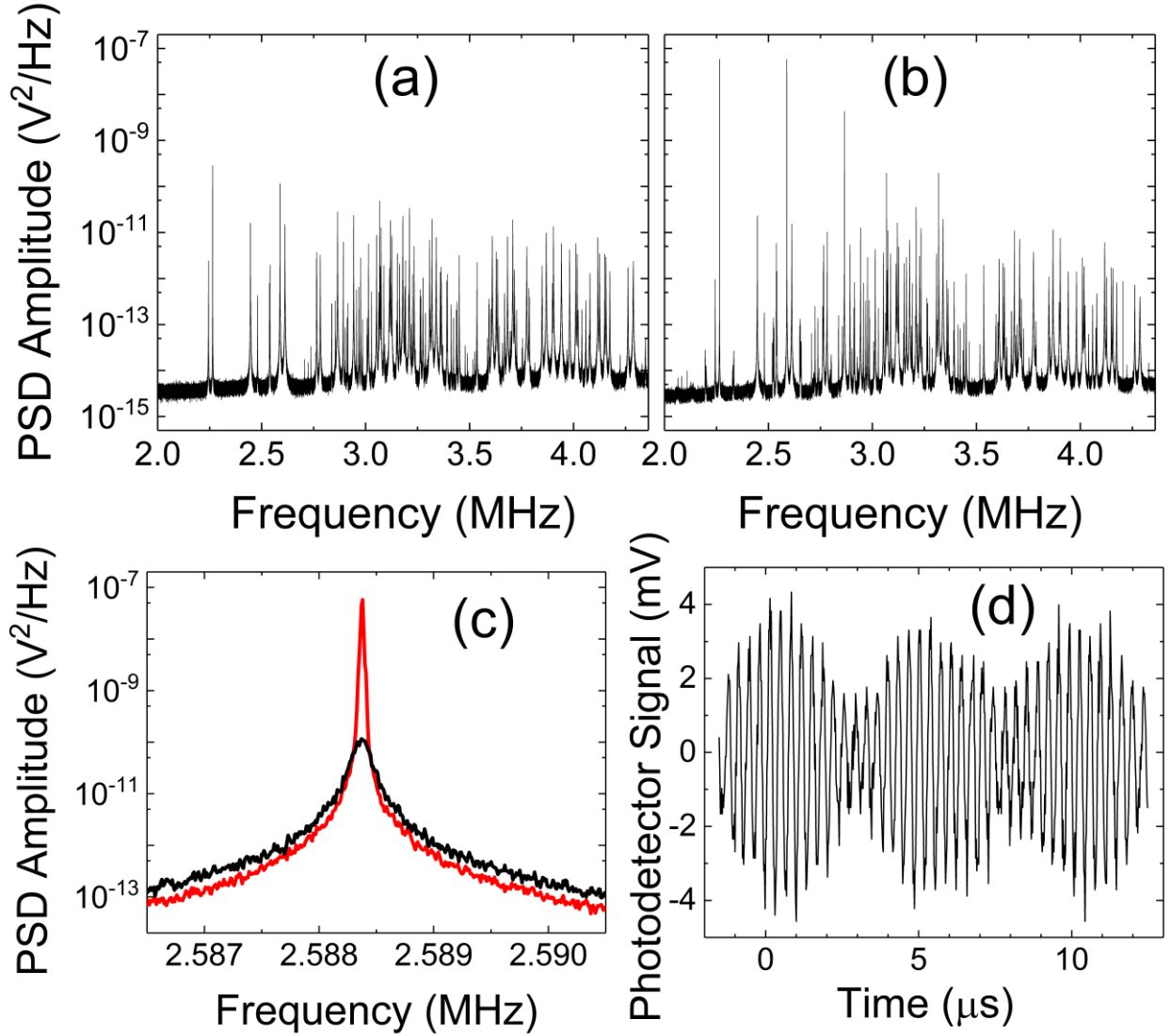


Figure 4. (a) PSD showing thermally driven NW resonance peaks. (b) PSD when detected NW motion is fed back to the array via heat pulses from a blue laser. Several resonances are observed to be driven into spontaneous self-sustained oscillations while others are decreased in amplitude, as expected depending upon the feedback phase. (c) A close look at a frequency region showing a single NW peak with (red curve) and without (black curve) feedback applied. The peak without feedback has a FWHM of about 170 Hz or Q of about 15,000, while the peak with feedback has a FWHM of about 12 Hz or Q of about 200,000. (d) Time record of the photodetector signal when two NW resonances are simultaneously driven into feedback oscillation. A clear beat note between resonances at 2.86 MHz and 3.07 MHz indicates simultaneous oscillation of the NW modes.

In summary, we have demonstrated the ability to grow 2D arrays of GaN NWs designed to coherently scatter light in a controlled fashion. We have shown that the selective-area grown NWs studied here are of similarly high quality compared to previously investigated random growth GaN NWs. Our system allows for the simultaneous measurement of the mechanical properties of all NWs in an array using a simple optical technique and without the need for any externally applied drive. Thus we are able to simultaneously monitor a collection of hundreds of nano-mechanical resonators, with Q factors comparable to commercial quartz resonators, contained within an area of 10-100 μm^2 . Arrays of GaN NWs, read out in this way, have promise for a variety of high sensitivity and spatially resolved sensing applications and as miniaturized NW-based clocks and frequency sources.

We gratefully acknowledge support for these studies by the National Institute of Standards and Technology (NIST) under award number 70NANB15H352 and by a Research & Innovation Seed Grant from the University of Colorado Boulder.

- (1) Jensen, K.; Kim, K.; Zettl, A. An Atomic-Resolution Nanomechanical Mass Sensor. *Nat. Nanotechnol.* 2008, 3 (9), 533–537.
- (2) Ekinci, K. L.; Huang, X. M. H.; Roukes, M. L. Ultrasensitive Nanoelectromechanical Mass Detection. *Appl. Phys. Lett.* 2004, 84 (22), 4469–4471.
- (3) Teufel, J. D.; Donner, T.; Li, D.; Harlow, J. W.; Allman, M. S.; Cicak, K.; Sirois, A. J.; Whittaker, J. D.; Lehnert, K. W.; Simmonds, R. W. Sideband Cooling of Micromechanical Motion to the Quantum Ground State. *Nature* 2011, 475 (7356), 359–363.
- (4) Teufel, J. D.; Donner, T.; Castellanos-Beltran, M. A.; Harlow, J. W.; Lehnert, K. W. Nanomechanical Motion Measured with an Imprecision below That at the Standard Quantum Limit. *Nat. Nanotechnol.* 2009, 4 (12), 820–823.
- (5) Hoch, S. W.; Montague, J. R.; Bright, V. M.; Rogers, C. T.; Bertness, K. A.; Teufel, J. D.; Lehnert, K. W. Non-Contact and All-Electrical Method for Monitoring the Motion of Semiconducting Nanowires. *Appl. Phys. Lett.* 2011, 99 (5), 3–6.
- (6) Tanner, S. M.; Gray, J. M.; Rogers, C. T.; Bertness, K. A.; Sanford, N. A. High-Q GaN Nanowire Resonators and Oscillators. *Appl. Phys. Lett.* 2007, 91 (20), 1–3.
- (7) Montague, J. R.; Dalberth, M.; Gray, J. M.; Seghete, D.; Bertness, K. A.; George, S. M.; Bright, V. M.; Rogers, C. T.; Sanford, N. A. Analysis of High-Q, Gallium Nitride Nanowire Resonators in Response to Deposited Thin Films. *Sensors Actuators, A Phys.* 2011, 165 (1), 59–65.

- (8) Montague, J. R.; Bertness, K. A.; Sanford, N. A.; Bright, V. M.; Rogers, C. T. Temperature-Dependent Mechanical-Resonance Frequencies and Damping in Ensembles of Gallium Nitride Nanowires. *Appl. Phys. Lett.* 2012, 101 (17).
- (9) Gray, J. M.; Rogers, C. T.; Bertness, K. A.; Sanford, N. A. Gallium Nitride Nanowire Electromechanical Resonators with Piezoresistive Readout. *J. Vac. Sci. Technol. B, Nanotechnol. Microelectron. Mater. Process. Meas. Phenom.* 2011, 29 (5), 52001.
- (10) Brubaker, M. D.; Duff, S. M.; Harvey, T. E.; Blanchard, P. T.; Roshko, A.; Sanders, A. W.; Sanford, N. A.; Bertness, K. A. Polarity-Controlled GaN/AlN Nucleation Layers for Selective-Area Growth of GaN Nanowire Arrays on Si(111) Substrates by Molecular Beam Epitaxy. *Cryst. Growth Des.* 2016, 16 (2), 596–604.
- (11) Bertness, K. A.; Roshko, A.; Mansfield, L. M.; Harvey, T. E.; Sanford, N. A. Mechanism for Spontaneous Growth of GaN Nanowires with Molecular Beam Epitaxy. *J. Cryst. Growth* 2008, 310 (13), 3154–3158.
- (12) Nowak, R.; Pessa, M.; Suganuma, M.; Leszczynski, M.; Grzegory, I.; Porowski, S.; Yoshida, F. Elastic and Plastic Properties of GaN Determined by Nano-Indentation of Bulk Crystal. *Appl. Phys. Lett.* 1999, 75 (14), 2070–2072.
- (13) Carr, D. W.; Evoy, S.; Sekaric, L.; Craighead, H. G.; Parpia, J. M. Measurement of Mechanical Resonance and Losses in Nanometer Scale Silicon Wires. *Appl. Phys. Lett.* 1999, 75 (7), 920–922.
- (14) Ilic, B.; Krylov, S.; Craighead, H. G. Theoretical and Experimental Investigation of Optically Driven Nanoelectromechanical Oscillators. *J. Appl. Phys.* 2010, 107 (3).
- (15) Belov, M.; Quitarano, N. J.; Sharma, S.; Hiebert, W. K.; Kamins, T. I.; Evoy, S. Mechanical Resonance of Clamped Silicon Nanowires Measured by Optical Interferometry. *J. Appl. Phys.* 2008, 103 (7).
- (16) Hwang, J.; Moerner, W. E. Interferometry of a Single Nanoparticle Using the Gouy Phase of a Focused Laser Beam. *Opt. Commun.* 2007, 280 (2), 487–491.
- (17) Walia, J.; Dhindsa, N.; Khorasaninejad, M.; Saini, S. S. Color Generation and Refractive Index Sensing Using Diffraction from 2D Silicon Nanowire Arrays. *Small* 2014, 10 (1), 144–151.
- (18) Khodadad, I.; Dhindsa, N.; Saini, S. S. Refractometric Sensing Using High-Order Diffraction Spots From Ordered Vertical Silicon Nanowire Arrays Refractometric Sensing Using High-Order Diffraction Spots From Ordered Vertical Silicon Nanowire Arrays. *IEEE Photonics J.* 2016, 8 (2), 4501010.
- (19) Ashcroft, N. W.; Mermin, N. D. *Solid State Physics*; 1976.

- (20) Cleland, A. N. *Foundations of Nanomechanics : From Solid-State Theory to Device Applications*; Springer: Berlin ; New York, 2003.
- (21) Hao, Z. L.; Erbil, A.; Ayazi, F. An Analytical Model for Support Loss in Micromachined Beam Resonators with in-Plane Flexural Vibrations. *Sensors and Actuators a-Physical* 2003, 109 (1–2), 156–164.
- (22) Ekinci, K. L.; Yang, Y. T.; Roukes, M. L. Ultimate Limits to Inertial Mass Sensing Based upon Nanoelectromechanical Systems. *J. Appl. Phys.* 2004, 95 (5), 2682–2689.